



## The shape dependence of magnetic and microwave properties for Ni nanoparticles

Fei Ma\*, Ji Ma, Juanjuan Huang, Jiangong Li\*

*Institute of Materials Science and Engineering, Lanzhou University, Lanzhou 730000, China*

### ARTICLE INFO

#### Article history:

Received 20 April 2011

Received in revised form

20 July 2011

Available online 11 August 2011

#### Keywords:

Wet-chemical synthesis

Shape anisotropy

Complex permeability

Microwave absorption

### ABSTRACT

The magnetic and microwave properties of Ni nanospheres and conical nanorods have been investigated through experimental and theoretical methods. Ni nanospheres and conical nanorods have the same crystal structure and close particle size, whereas the remanence ratio, coercivity, dynamic permeability and microwave absorbing properties show great dependence on their shape. Ni conical nanorods self-assembled into urchin-like structure have higher natural resonance frequency due to the large shape anisotropy compared to the Ni nanospheres. Supposing random spatial distribution of magnetic easy axes and using the Landau–Lifshitz–Gilbert equation associated with the Bruggeman's effective medium theory, we simulate the complex permeability of Ni nanoparticles, which agrees well with the experimental results.

© 2011 Elsevier B.V. All rights reserved.

Ferromagnetic metals have been paid much attention in microwave application due to their higher saturation magnetization and permeability compared to ferrite. Such materials which were expected as high density recording media, magnetic field sensor or electromagnetic wave absorption material should have high value of complex permeability, tunable resonance frequency and low eddy current loss in microwave range [1–5]. Considerable works have investigated the complex permeability of metal-based magnetic material through experimental or theoretical method. It is widely proved that the magnetic properties and microwave properties of ferromagnetic nanoparticles are related to their size and shapes [6–8]. As the particle size decreases, eddy current loss can be considerably suppressed and when it comes into nanometer scale, surface effect [9], size effect [10,11] combined with shape anisotropic effect [12–14] become dominant in the magnetic and microwave properties. The behavior of the complex permeability in microwave frequency should ascribe to such mixed effect to clarify which we should find a proper way to separate the size, surface and shape effect. In our present work, we compared Ni nanospheres with Ni conical nanorods to research the shape effect on the static magnetic properties (coercivity and remanence ratio), complex permeability and microwave absorbing properties. Landau–Lifshitz–Gilbert equation associated with the Bruggeman's effective medium theory were used to simulate the complex permeabilities of Ni nanospheres and conical nanorods supposing random spatial distribution of magnetic easy axes.

To prepare Ni nanospheres, 25 ml alcoholic solution of 0.1 M  $\text{NiCl}_2 \cdot 6\text{H}_2\text{O}$ , 25 ml alcoholic solution with 0.2 g polyvinyl pyrrolidone (PVP,  $K=30$ ), 50 ml alcoholic solution of 0.5 M NaOH and 6 ml hydrate hydrazine ( $\text{N}_2\text{H}_4 \cdot \text{H}_2\text{O}$  80%) were mixed together. Then, the mixed solution was heated to 80 °C for 3 h. After washing and desiccation, the spherical Ni nanoparticles were obtained. To prepare Ni conical nanorods, 25 ml alcoholic solution of 0.1 M  $\text{NiCl}_2 \cdot 6\text{H}_2\text{O}$  and 25 ml alcoholic solution with 0.2 g PVP were mixed, and 6 ml hydrate hydrazine was added into the above solution dropwise at 70 °C. A pink suspension was obtained immediately. The as-prepared suspension was added dropwise into a mixed solution with 50 ml alcoholic solution of 0.5 M NaOH and 10 ml hydrate hydrazine in a three-necked flask at 80 °C. Then, the solution was refluxed for 3 h. After washing and desiccation, Ni conical nanorods self-assembled into urchin-like structure were obtained.

The scanning electron microscopy (SEM) observations were carried out to investigate the morphology of Ni nanoparticles. Ni nanospheres with a mean diameter of 30–50 nm are shown in Fig. 1(a) while conical nanorods radially growing from one center into urchin-like architectures are shown in Fig. 1(b). The nanorods have diameters in the range of 25–50 nm and lengths up to 500 nm. Fig. 1(c) shows the X-ray diffraction (XRD) patterns of the as-prepared Ni nanospheres and conical nanorods. All diffraction peaks can be indexed with the face-centered cubic (fcc) Ni. No additional diffraction peaks from the impurities such as nickel oxide or hydroxide were detected. The broad diffraction peaks, which are quantified by the full-width at half-maximum (FWHM) are indicative of the ultrafine Ni particles. Furthermore, the average grain dimensions are estimated to be 30 nm for nanospheres and 35 nm

\* Corresponding authors.

E-mail addresses: maf@lzu.edu.cn (F. Ma), lijg@lzu.edu.cn (J. Li).

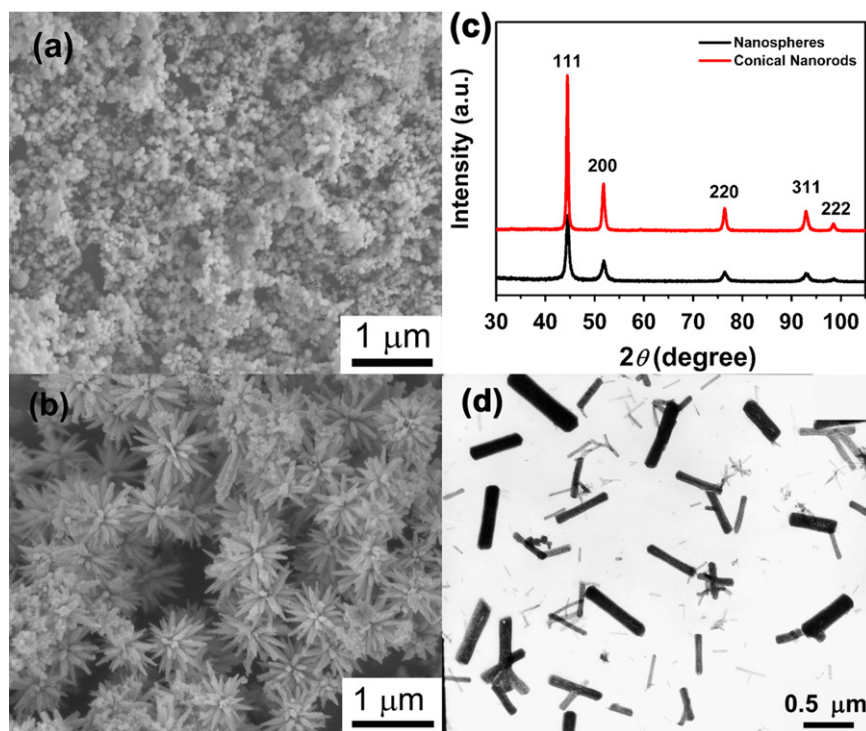


**Fig. 1.** The SEM micrographs of Ni nanospheres (a) and conical nanorods (b); XRD patterns of the Ni nanospheres and conical nanorods (c); TEM micrograph of the as-synthesized coordination compound (d).

for conical nanorods with the FWHM (with the instrumental peak width eliminated) of the (111), (200) and (220) crystallographic planes according to the Scherrer equation. The calculated grain sizes are consistent with the diameters of nanospheres and nanorods, which suggests that both the Ni nanospheres and the conical nanorods obtained by wet chemical methods are single crystal.

It was found that the adding sequence of the reactants plays a dominant role in the control of crystal morphology. The adding sequence of the reactants dominated the formation of intermediates in the reduction procedure. Conical rods were not obtained unless the intermediate known as coordination compound  $\text{Ni}(\text{N}_2\text{H}_4)_x\text{Cl}_2$  was formed through the reduction reaction. To research the mechanism of the formation of conical nanorods, we investigated the morphology and composition of the intermediate. It is found that the probable chemical formula is  $\text{Ni}(\text{N}_2\text{H}_4)_3\text{Cl}_2$  based on the weight percentages of 26.17, 37.44 and 5.34 wt% for Ni, N and H, respectively, by atomic emission spectrometer and elemental analysis. Fig. 1(d) shows the transmission electron microscopy (TEM) observations of the  $\text{Ni}(\text{N}_2\text{H}_4)_3\text{Cl}_2$  synthesized at 70 °C. All particles are rod-like maintaining diameters about 100–300 nm and lengths up to 400–600 nm. The formation of coordination compound is probably attributed to the nature of the electrostatic attraction. As we know, each nitrogen in hydrazine has a couple of unbonded electrons, so that hydrazine is eager to absorb positive charged ions such as  $\text{Ni}^{2+}$ . It is reasonable to conclude that such rod-like coordination compound can serve as an in-situ template resulting in the Ni conical nanorods. However, the bond energy of  $\text{OH}^-$  and  $\text{Ni}^{2+}$  is larger than that of  $\text{N}_2\text{H}_4$  and  $\text{Ni}^{2+}$  so that the rod-like coordination compound can only be ensured by adding  $\text{N}_2\text{H}_4 \cdot \text{H}_2\text{O}$  first into the  $\text{NiCl}_2$  solution, and without the rod-like coordination compound as the precursor, Ni conical nanorods cannot be synthesized.

The  $M-H$  hysteresis loops of the Ni nanospheres and nanorods are illustrated in Fig. 2(a). It can be seen that they are both ferromagnetic and their coercivity ( $H_c$ ) and remanence ratio

( $M_r/M_s$ ) are 134 Oe, 0.32 and 279 Oe, 0.38, respectively. The  $H_c$  and  $M_r/M_s$  of the Ni conical nanorods are both higher than that of the Ni nanospheres. Considering that the nanospheres and conical nanorods have close grain size and particle diameter, such discrepancy in  $H_c$  and  $M_r/M_s$  is probably due to the effect of shape anisotropy. As we know, the effective anisotropy, which is the sum of magnetocrystalline and shape anisotropy, is directly proportional to the coercivity. Along long axis of the nanorods the demagnetizing field is much smaller compared to that of short axis, which means the pinning of the magnetization in the long axis direction. Such pinning effect usually makes the magnetization harder to reverse so that higher  $H_c$  and  $M_r/M_s$  compared to isotropic structures. This is why the  $H_c$  and  $M_r/M_s$  of Ni conical nanorods is higher than that of Ni nanospheres.

The saturation magnetization of the bulk Ni at 300 K is 55.0 emu/g [15]. Both of the saturation magnetizations of nanospheres (45.02 emu/g) and nanorods (43.77 emu/g) are smaller than that of bulk Ni. There are several reasons for the decrease in  $M_s$  such as the surface oxidation, the nonmagnetic or weakly magnetic interfaces [16], the ligand effect on the particle surface, etc. It was inevitable to have oxidation layers for ultra fine nanoparticles in our present work. The oxide layer of the Ni particle is an antiferromagnet, so that the presence of such layers usually has no contribution to the  $M_s$  and lowers the magnetic moment per unit mass, and the spin of nickel which is close to the oxide layer is pinned due to the exchange anisotropy interaction between the antiferromagnetic layer of NiO and the ferromagnetic core of Ni [17]. Furthermore, poor magnetic properties found for nanoparticles were usually related to the presence of precursor residues coordinated on the surface. It is well known that strong  $\pi$ -acceptor ligands, such as carbon monoxide, induce a dramatic collapse of the saturation magnetization [18,19]. In our experimental system, PVP which is a widely used surfactant serves as a dispersant. It usually absorbs on the surface of Ni nanoparticles, so that the saturation magnetization might also decrease through the ligand effect of carbonyl groups in PVP.

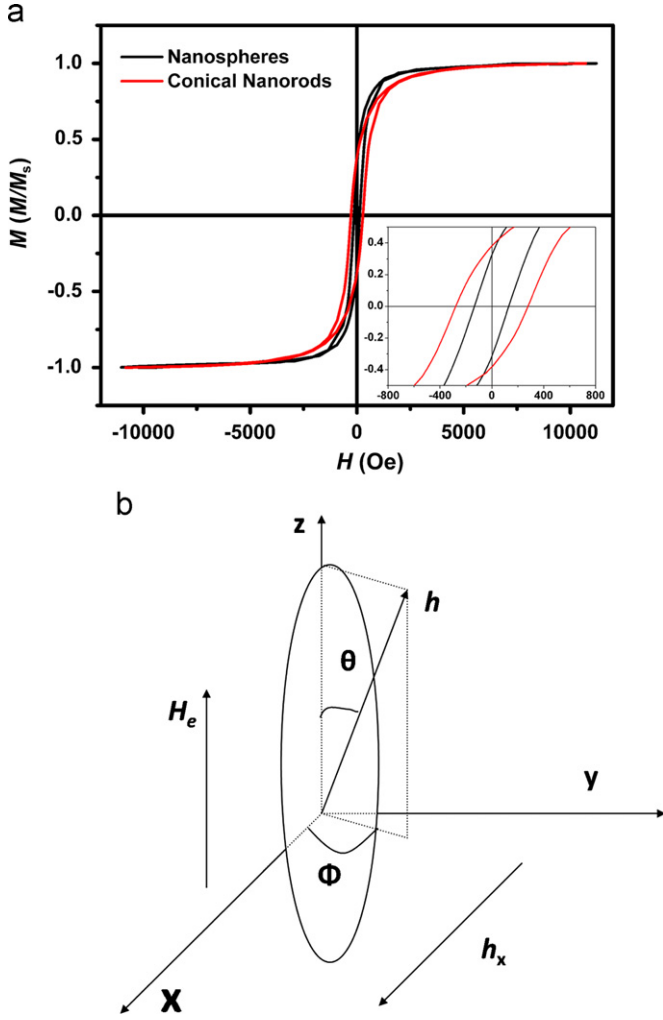


Fig. 2. Magnetic hysteresis loops of the Ni nanospheres and conical nanorods (a); coordinate system for microwave propagation in a single anisotropic particle (b).

The microwave permeability of the Ni nanoparticle–paraffin wax composites compacted into ring shapes was measured. The composites with 21.0 vol% Ni nanospheres and 23.3 vol% Ni conical nanorods were investigated, respectively, in the range of 0.1–18 GHz by measuring the reflection coefficient  $S_{11}$  and the transmission coefficient  $S_{21}$  in an APC7 coaxial mode. Fig. 3 (triangle lines) shows the frequency dependence of complex permeability ( $\mu'$  and  $\mu''$ ) in the range of 0.1–18 GHz. The complex permeability for Ni nanospheres and conical nanorods has similar pattern:  $\mu'$  decrease with frequency, while  $\mu''$  of the composites show a broad resonance peak, which is 2.8 GHz for nanospheres and 4.3 GHz for conical nanorods. In gigahertz range, the resonance behavior for metal magnetic nanoparticles is usually ascribed to the natural resonance.

For the calculation of dynamic frequency dependent permeability around natural resonance range, Gilbert equation has been widely used:

$$\frac{dM}{dt} = -\gamma M \times H_e + \frac{\alpha}{M_s} M \times \frac{dM}{dt} \quad (1)$$

where  $M$  is the magnetization,  $H_e$  is the effective anisotropic field,  $\gamma$  is the gyromagnetic factor,  $\alpha$  is the damping coefficient and  $M_s$  is the saturation magnetization. When the microwave field  $h$  is perpendicular to the effective anisotropic field (the diagram

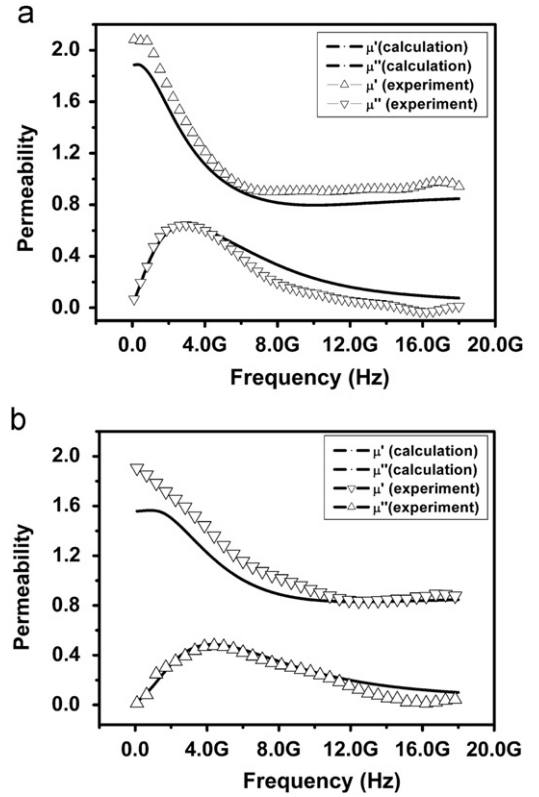


Fig. 3. Comparison of experimental and calculated complex permeability for Ni nanospheres (a) and conical nanorods (b).

is shown in Fig. 2(b)), the magnetization and field are given as

$$M = (m_x, m_y, M_s) \\ H = (h_x, 0, H_e) \quad (2)$$

By substituting Eq. (2) into Eq. (1), considering  $|h_x| \ll |H_e|$  and  $|m| \ll |M_s|$ , the diagonal element  $\mu$  and off diagonal element  $\kappa$  are as follows:

$$\mu = 1 + \frac{m_x}{h_x} = 1 + \frac{\omega_m(\omega_0 + i\alpha\omega)}{(\omega_0 + i\alpha\omega)^2 - \omega^2} \\ \kappa = \frac{m_y}{h_x} = \frac{-\omega_m\omega}{(\omega_0 + i\alpha\omega)^2 - \omega^2} \quad (3)$$

where  $\omega_m = \gamma M_s$  and  $\omega_0 = \gamma H_e$ . The above solutions were deduced based on the microwave field  $h$  perpendicular to  $H_e$ . When the microwave field  $h$  is not perpendicular to  $H_e$ , by substituting Eq. (2) into Eq. (1) and combining with Maxwell's equations, the permeability tensor is given by [20]

$$\mu = \frac{1}{\epsilon} \left( \frac{\delta}{i\omega} \right)^2 \begin{pmatrix} 1 - \sin^2\theta \cos^2\phi & -\sin^2\theta \sin\phi \cos\phi & -\sin\theta \cos\theta \cos\phi \\ -\sin^2\theta \sin\phi \cos\phi & 1 - \sin^2\theta \sin^2\phi & -\sin\theta \cos\theta \sin\phi \\ -\sin\theta \cos\theta \cos\phi & -\sin\theta \cos\theta \sin\phi & 1 - \cos^2\theta \end{pmatrix} \\ \delta = i\omega(\mu_0\epsilon)^{1/2} \left\{ \frac{(\mu^2 - \kappa^2)\sin^2\theta + 2\mu \pm [(\mu^2 - \kappa^2)^2 \sin^4\theta + 4\kappa^2 \cos^2\theta]^{1/2}}{2[(\mu-1)\sin^2\theta + 1]} \right\}^{1/2} \quad (4)$$

where  $\delta$  is given in Eq. (5) and  $\mu$  and  $\kappa$  are given in Eq. (3). Eq. (4) can be used to calculate the intrinsic permeability ( $\mu_i$ ) of one magnetic domain. With a random distribution of  $H_e$  an equivalent average magnetic permeability should be given as follows, in which 10,000 single domains with randomly generated angles  $\theta$

and  $\varphi$  were considered.

$$\langle \mu_i \rangle = \frac{\sum_1^N \mu_i(\theta, \phi)}{N} \quad (6)$$

An equivalent scalar permeability of  $\mu_i$  can then be calculated by taking the Eigen value of the permeability tensor:

$$\mu_i = \text{Eigenvalue}(\langle \mu_i \rangle) \quad (7)$$

Magnetic particles with certain volume fraction  $P$  are dispersed in a nonmagnetic matrix (paraffin wax). The effective permeability ( $\mu_{eff}$ ) for composite can be calculated by normal Bruggeman's effective medium theory [21,22]

$$p \frac{\mu_i - \mu_{eff}}{\mu_i + 2\mu_{eff}} + (1-p) \frac{1 - \mu_{eff}}{1 + 2\mu_{eff}} = 0 \quad (8)$$

Fig. 3 (solid lines) shows theoretical fitting curves of the complex permeability for Ni nanospheres (Fig. 3(a)) and Ni conical nanorods (Fig. 3(b)). We suppose that the saturation magnetization  $4\pi M_s$  is 4.90 kG based on the experimental data of VSM for both nanospheres and nanorods, the damping parameters are 0.50 for nanospheres and 0.65 for nanorods from the width of the natural resonance peak. It was found that the fitting curves match satisfactorily with the experimental data when the  $H_e = 0.187$  kOe for nanospheres and 0.700 kOe for conical nanorods. The  $H_e$  of Ni conical nanorods is much higher than that of Ni nanospheres, which shows good agreement with the discussion on  $H_c$ . Moreover, from the Kittel [8] model for natural resonance, the natural resonance peak varies linearly with  $H_e$ , which is the sum of crystalline anisotropy, shape anisotropy, surface anisotropy, etc. In our case, Ni nanospheres and conical nanorods have the same crystal structure and close particle size, so that the major difference between the two samples is their morphology. Ni conical nanorods have larger shape anisotropy which originated from demagnetization effect can increase  $H_e$  dramatically. This is why Ni conical nanorods have larger  $H_e$  and higher resonance frequency compared to Ni nanospheres.

In order to explore the microwave absorbing properties of the composites, both magnetic and dielectric loss should be considered. As shown in Fig. 4(a), the complex permittivity of Ni nanoparticles

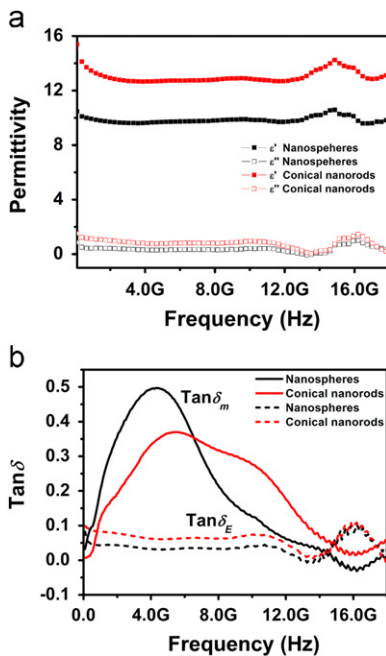


Fig. 4. Frequency dependences of the complex permittivity (a); frequency dependences of the dielectric and magnetic loss tangent (b).

was plotted as a function of frequency. The real part  $\epsilon'$  and imaginary part  $\epsilon''$  of the complex permittivity maintained almost a constant over 0.1–18 GHz except for the little fluctuation above 14 GHz. It was found that the complex permittivity for nanorods was higher than that of nanospheres. In the metal–insulator composites, the space charge and the dipole polarization could be ascribed to the polarization phenomena. The space charge polarization often takes place in the interface between the metal core and the insulator matrix. The free electrons from the metal fractions promote the charge accumulation at the interfaces and the higher permittivity is attained due to the improved electrical conductivity. Nanorods have larger specific surface area, which might result to more space charge polarization so that higher complex permittivity compared to nanospheres. The dielectric and magnetic loss tangent can be expressed as  $\tan \delta_E = \epsilon''/\epsilon'$  and  $\tan \delta_M = \mu''/\mu'$ , respectively, which means the ratio of energy loss to the energy storage. Fig. 4(b) shows frequency dependence of the dielectric and magnetic loss tangent of Ni nanospheres and conical nanorods composites. It can be seen that the value of magnetic loss is much higher than that of dielectric loss, illustrating that the main loss for the composites in the range of 0.1–18 GHz is magnetic loss. Furthermore, the magnetic loss tangent appears peaks with the increase of frequency. The peak for the nanospheres has the maximum value about 0.5 higher than that of conical nanorods. However, the peaks for conical nanorods are wider and appear in higher frequency range compared to that of nanospheres, which means conical nanorods might be more suitable to be a broad band microwave absorber.

The reflection loss (RL) of a microwave absorbing layer backed by a perfect conductor was calculated by the following equations:

$$RL(\text{dB}) = 20 \log_{10} \left| \frac{Z_{in} - 1}{Z_{in} + 1} \right| \quad (9)$$

$$Z_{in} = \left( \frac{\mu_r}{\epsilon_r} \right)^{1/2} \tanh \left[ j \left( \frac{2\pi f d}{c} \right) (\mu_r \epsilon_r)^{1/2} \right] \quad (10)$$

where RL is a ratio of reflected power to incident power in dB,  $Z_{in}$  is the normalized input impedance relative to the impedance in free space,  $\epsilon_r = \epsilon' - j\epsilon''$  and  $\mu_r = \mu' - j\mu''$  is the complex permittivity and complex permeability of the absorber material,  $d$  is the thickness of the absorber, and  $c$  and  $f$  are the velocity of light and the frequency of microwave in free space, respectively. The RL curves were shown in Fig. 5 for both Ni nanospheres and conical nanorods. The RL was less than  $-10$  dB in the 6.7–9.5 GHz for conical nanorods while more than  $-8$  dB in the whole frequency range for nanospheres with thickness of 2.5 mm. The values less than  $-10$  dB indicates that more than 90% of the introduced microwaves are absorbed, so this value is the target value to be attained for the absorber's applications. More importantly, the thickness of the sample is smaller than that of the usual ferrite material indicating that the Ni conical nanorods may be good microwave absorption filler in broad frequency band.

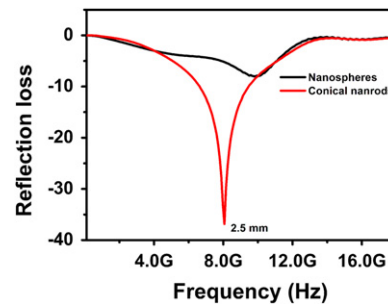


Fig. 5. Simulated RL for Ni nanoparticle–paraffin wax composites with the thickness of 2.5 mm.

In conclusion, the Ni nanospheres and conical nanorods have been synthesized by wet-chemical methods. The anisotropic growth of Ni nanoparticles should be ascribed to the formation of one-dimensional intermediate  $\text{Ni}(\text{N}_2\text{H}_4)_3\text{Cl}_2$ . The synthesized Ni nanospheres and conical nanorods have close particle and grain size, which makes them the ideal candidate to investigate the shape effect on their magnetic properties. We compared the magnetic and microwave properties of the Ni nanospheres and conical nanorods by both experimental and theoretical methods. The coercivity, remanence ratio and natural resonance frequency of Ni nanoparticles all show dependence on their shape. Ni conical nanorods with larger shape anisotropy compared to nanospheres have larger coercivity and higher resonance frequency.

This work was supported by Open Project of Key Laboratory for Magnetism and Magnetic Materials of the Ministry of Education, Lanzhou University (LZUMMM2011001) and the Fundamental Research Funds for the Central Universities (lzujbky-2011-60).

## References

- [1] M. Darques, J. Medina, L. Piraux, L. Cagnon, I. Huynen, *Nanotechnology* 21 (2010) 145208.
- [2] S.A. Bender, Y. Tserkovnyak, A. Brataas, *Phys. Rev. B* 82 (2010) 180403.
- [3] X.F. Zhang, X.L. Dong, H. Huang, Y.Y. Liu, W.N. Wang, X.G. Zhu, B. Lv, J.P. Lei, C.G. Lee, *Appl. Phys. Lett.* 89 (2006) 053115.
- [4] B. Wang, J. Wei, Y. Yang, T. Wang, F. Li, *J. Magn. Magn. Mater.* 323 (2011) 1101.
- [5] R. Che, L. Peng, X. Duan, Q. Chen, X. Liang, *Adv. Mater.* 16 (2004) 401.
- [6] A. Aharoni, *J. Appl. Phys.* 69 (1991) 7762.
- [7] A. Aharoni, *J. Appl. Phys.* 81 (1997) 830.
- [8] C. Kittel, *Phys. Rev.* 73 (1948) 155.
- [9] J. Ma, J. Li, X. Ni, X. Zhang, J. Huang, *Appl. Phys. Lett.* 95 (2009) 102505.
- [10] P. Toneguzzo, G. Viau, O. Acher, F. Fiévet-Vincent, F. Fiévet, *Adv. Mater.* 10 (1998) 1032.
- [11] D. Mercier, J.-C.S. Lévy, G. Viau, F. Fiévet-Vincent, F. Fiévet, P. Toneguzzo, O. Acher, *Phys. Rev. B* 62 (2000) 532.
- [12] X. Kou, X. Fan, H. Zhu, R. Cao, J. Xiao, *IEEE Trans. Magn.* 46 (2010) 1143.
- [13] F. Ma, Y. Qin, Y. Li, *Appl. Phys. Lett.* 96 (2010) 202507.
- [14] F. Ma, J. Huang, J. Li, Q. Li, *J. Nanosci. Nanotechnol.* 9 (2009) 3219.
- [15] J.H. Hwang, V.P. Dravid, M.H. Teng, J.J. Host, B.R. Elliott, D.L. Johnson, T.O. Mason, *J. Mater. Res.* 12 (1997) 1076.
- [16] D.H. Chen, C.H. Hsieh, *J. Mater. Chem.* 12 (2002) 2412.
- [17] Y. Du, M. Xu, J. Wu, Y. Shi, H. Lu, R. Xue, *J. Appl. Phys.* 70 (1991) 5903.
- [18] J. Osuna, D. Caro, C. Amiens, B. Chaudret, E. Snoeck, M. Respaud, J. Broto, A. Fert, *J. Phys. Chem.* 100 (1996) 14571.
- [19] N. Cordente, M. Respaud, F. Senocq, M. Casanove, C. Amiens, B. Chaudret, *Nano Lett.* 1 (2001) 565.
- [20] L.Z. Wu, J. Ding, H.B. Jiang, C.P. Neo, L.F. Chen, C.K. Ong, *J. Appl. Phys.* 99 (2006) 083905.
- [21] A. Sihvola, *Electromagnetic Mixing Formulas and Applications*, Institution of Electrical Engineers, London, 1999.
- [22] L. Olmedo, G. Chateau, C. Deleuze, J.L. Forveille, *J. Appl. Phys.* 73 (1993) 6992.